



Spatial correlation among cultivated land intensive use and carbon emission efficiency: A case study in the Yellow River Basin, China

Xiao Zhou^{1,2} · Juan Yu^{1,2} · Jiangfeng Li^{1,2} · Shicheng Li^{1,2} · Dou Zhang³ · Di Wu^{1,2} · Sipei Pan^{1,2} · Wanxu Chen^{4,5,6,7}

Received: 14 October 2021 / Accepted: 23 January 2022 / Published online: 30 January 2022
© The Author(s), under exclusive licence to Springer-Verlag GmbH Germany, part of Springer Nature 2022

Abstract

Considering the current global goal of carbon neutrality, the relationship between cultivated land intensive use (CLIU) and carbon emission efficiency (CEE) should be explored to address the global climate crisis and move toward a low-carbon future. However, previous work in this has been conducted at provincial/regional scales and few have identified the spatial correlation between CLIU and CEE at the scale of large river basins. Therefore, this study explored the spatiotemporal characteristics of CLIU, cultivated land carbon emissions (CLCE), and CEE, as well as the spatial correlation between CLIU and CEE in the Yellow River Basin (YRB), China. A comprehensive evaluation model, the Intergovernmental Panel on Climate Change (IPCC) coefficient methodology, existing data envelopment analysis model, and bivariate spatial autocorrelation models were used to analyze statistical data from 2005 to 2017. We found that the overall CLIU and CLCE values in the YRB exhibited a continuous increase; the average carbon emission total efficiency and carbon emission scale efficiency first decreased and then increased, and the average carbon emission pure technical efficiency gradually decreased. Areas of high CLCE were concentrated in eastern areas of the YRB, whereas those of high CLIU, carbon emission total efficiency, carbon emission scale efficiency, and carbon emission pure technical efficiency predominantly appeared in the eastern areas, followed by central and western areas of the YRB. Spatial analysis revealed a significant spatial dependence of CLIU on CEE. From a global perspective, the spatial correlations between CLIU and CEE changed from positive to negative with time. Moreover, the aggregation degree between CLIU and CEE gradually decreases with time, while the dispersion degree increases with time, and the spatial correlation gradually weakens. The local spatial autocorrelation further demonstrates that the number of high–low and low–high clusters between CLIU and CEE gradually increases over time, while the number of high–high and low–low clusters gradually decreased over time. Collectively, these findings can help policymakers formulate feasible low-carbon and efficient CLIU policies to promote win–win cooperation among regions.

Keywords Cultivated land intensive use · Carbon emission efficiency · Spatial analysis · Sustainable development · Yellow River Basin · China

Introduction

The current goal of carbon neutrality is driving low-carbon cultivated land use in China. Moreover, the growing population and shrinking cultivated land area is driving improvements in the intensive use of cultivated land (Bajan and Mrowczynska-Kaminska, 2020; Ge et al., 2018). Such transformations can make cultivated land use more energy efficient (Fox et al., 2019) and enhance environmental protection (Han and Zhang, 2020). However, previous similar work has been conducted at provincial/regional scales with few identifying the spatial correlation between cultivated land intensive use (CLIU) and carbon emission efficiency (CEE) at the scale of large river basins. This is not conducive

Responsible Editor: Philippe Garrigues

Highlights

- We evaluate cultivated land intensive use (CLIU) and carbon emission efficiency (CEE).
- Increased CLIU increases cultivated land carbon emissions and decreases CEE.
- CLIU and CEE exhibit significant spatial dependence in the Yellow River Basin.
- Spatial correlations between CLIU and CEE vary spatially and temporally.

✉ Wanxu Chen
cugcwx@cug.edu.cn

Extended author information available on the last page of the article

to broader national and regional cooperation for ensuring food security, reducing carbon dioxide emissions, and mitigating global warming in the future.

The Yellow River is the mother river of the Chinese nation, giving birth to the ancient and great Chinese civilization. As early as ancient times, the Yellow River Basin (YRB) was an important home for Chinese ancestors to breed and live (Su et al., 2000) and retains many traditional agricultural areas. Over the past 3000 years, the YRB has been the political, economic, and cultural center of China (Wang et al., 2018a, b). Currently, this region is characterized by agriculture and animal husbandry (Zhang et al., 2019), with major agricultural production areas, such as Huang-Huai-Hai Plain, Fen-Wei Plain, and Hetao irrigation area, accounting for one-third of China (Liu et al., 2021). The YRB has the largest population and agricultural scale of similar regions globally. However, the large-scale land planning and extensive development over the past 20 years have seriously threatened the YRB's ecological environment and water resources (Chen et al., 2021a, b, c; Lv et al., 2019; Zhang et al., 2021a, b, c), causing the disappearance of vast areas of high-quality cultivated land (Xiao et al., 2021). Therefore, in 2019, the central government promoted a national strategy for ecological protection and high-quality development of the YRB, requiring the area to prioritize ecology and pursue green development (Chen et al., 2020a, b, c). Accordingly, by 2030, the YRB aims to further enhance its water resource security capacity, significantly improve its ecological environment quality, and consolidate its position as a national food and energy base (Song et al., 2021). In the context of carbon neutrality, we hope to provide a region that balances economic development with environmental governance, food security, and ecological protection for countries and regions.

According to the classical theories, land intensive use includes the concentration of increased production capacity and living labor on a certain area of land using advanced technologies and management methods to obtain high yield and income (Liang and Li, 2020; Ricardo, 2001). The CLIU evolved from land intensive use and can be divided, based on production factor input, into capital intensive, labor intensive, and technology intensive (Sun et al., 2020). Scholars have gradually constructed a relatively complete CLIU research system that is transitioning from the macro- to microscales (Shang et al., 2019). Related studies have made significant advances in the index system (Liu et al., 2016), food security (Ge et al., 2018), driving mechanisms (Lou et al., 2017), spatial differences (Xie et al., 2016), negative environmental effects (Abe et al., 2020), sustainable intensification (Ameur et al., 2020), and other aspects of CLIU (Liu et al., 2020a, b, c; Xie et al., 2021). Moreover, the related research methods and models have diversified over time. For example, the comprehensive evaluation model (Huang et al.,

2021), analytic hierarchy process (Tercan and Dereli, 2020), factor analysis method (Zhang et al., 2021a, b, c), emergy method (Su and Fath, 2012), material flow (Xie et al., 2021), econometric model (Deng et al., 2015), coupling coordination degree model (Liu et al., 2020a, b, c), spatial econometric model (Rocha et al., 2019), geographically weighted regression model (Xu et al., 2020), and geographical detector model (Liu et al., 2020a, b, c) have all been widely used. Simultaneously, the research scale has also diversified, with most studies performed on macro- and mesoscales, i.e., for nations (Golosov et al., 2021), provinces (Liu et al., 2016), urban agglomerations (Dai et al., 2020), cities (Chen et al., 2021a, b, c), and counties (Chen et al., 2020b). These studies have laid a solid foundation for the generation of this study.

Carbon emission research fields include industry, agriculture, and services (Garba et al., 2021; Ma et al., 2019; Pendrill et al., 2019). Cultivated land carbon emission research is a branch of carbon emission research, covering spatiotemporal evolution (Cui et al., 2021), regional differences (Chuai et al., 2013), driving force mechanisms (Lal, 2020), and emission reduction potential (Garg et al., 2020). The research methods primarily include the Intergovernmental Panel on Climate Change (IPCC) coefficient methodology (Li et al., 2021a, b), as well as the system dynamics model (Liu et al., 2003), logarithmic mean Divisia index method (Chen et al., 2017), and linear programming method (Wang et al., 2015). Carbon emissions research is the basis of CEE research, which generally refers to the production relation ratio that minimizes carbon dioxide emissions and maximizes economic output with no increase in labor, capital, or energy input (Arneth et al., 2017). The primary analysis methods include data envelopment analysis (DEA) (Ibrahim et al., 2021), stochastic frontier analysis (Wanke et al., 2020), and regression analysis (Akram et al., 2021). Various CEE-based studies have expanded fields related to carbon emissions, including the comparison between CEE and total factor productivity (Zhou et al., 2019), CEE promotion path analysis (Ahmad et al., 2021), the interaction between CEE and economic development (Sarkodie and Ozturk, 2020), and the relationship between CEE and low-carbon agricultural production (Bajan and Mrowczynska-Kaminska, 2020). Collectively, these studies have provided important reference points for determining spatial correlations among CLIU and CEE.

Previous studies on the relationship between land use and carbon emissions have focused on the mechanism by which land use change impacts carbon emissions (Xu and Yang, 2019), land use structure and low-carbon optimization (Chuai et al., 2015), and land use carbon budget and carbon compensation (Kondo et al., 2020). Meanwhile, few studies have examined land intensive use and CEE, particularly between CLIU and CEE. The mechanism between CLIU and CEE may be superimposed by

their respective driving factors, as the driving mechanism of CLIU is interrelated and influenced by management measures, agricultural facilities, development stages, and education input (Fan et al., 2012; Grassini and Cassman, 2012; Ni et al., 2021; Xie et al., 2016). Meanwhile, the driving mechanism of CEE is restricted by capital, labor, technological level, industrial structure, and economic development level (Pan et al., 2020; Yang et al., 2021; Zhang and Chen, 2021). Therefore, the spatial correlation and aggregation among CLIU and CEE directly, or indirectly, reflect the superposition of the above drivers. Moreover, with the implementation of ecological civilization construction, returning cultivated land to forests and permanent basic cultivated land protection policies (Cheng et al., 2017; Wu et al., 2017; Zhu et al., 2021), while exploring the spatial correlations between CLIU and CEE, can provide insights regarding the effects of regional cultivated land use policies to facilitate the timely adjustment of identified deficiencies. Simultaneously, it can enhance the interaction and coordination of cultivated land use policies among regions and promote the balanced development of cultivated land use among regions.

Therefore, this research aimed to determine the spatial correlation degree and distribution patterns between CLIU and CEE in the YRB, China. From the perspective of a large river basin, we employed a comprehensive evaluation model, IPCC coefficient methodology, and the DEA method of Banker, Charnes, and Cooper (DEA-BCC) to measure the spatiotemporal characteristics of CLIU, CLCE, and CEE, respectively, in the YRB. Subsequently, bivariate spatial autocorrelation models were used to measure the spatial correlation between CLIU and CEE, and their spatial aggregation and differentiation characteristics were explored at the large river basin scale to address the current gaps in the literature. To this end, this study had four objectives: (1) to determine more comprehensive aspects of CLIU features at a large river basin scale; (2) to investigate whether CLCE has increased or decreased in the YRB; (3) to investigate the spatiotemporal characteristics of different types of CEE; (4) to reveal the spatial correlation between CLIU and CEE at both global and local levels on a large river basin scale. To achieve these objectives, this study addressed the following four research questions:

- (1) What are the spatiotemporal characteristics of prefecture-level CLIU in the YRB from 2005 to 2017?
- (2) What are the spatiotemporal characteristics of prefecture-level CLCE in the YRB from 2005 to 2017?
- (3) What are the spatiotemporal characteristics of prefecture-level CEE in the YRB from 2005 to 2017?
- (4) What is the spatial correlation between CLIU and CEE in the YRB from 2005 to 2017?

Data

Study area

The Yellow River is the second longest river in China, with a total length of 5,464 km. The river originates on the Qinghai–Tibet Plateau in the west and flows into the Bohai Sea in the east. The YRB has exerted an important influence on the origin and spread of agriculture in China (Yin et al., 2021) and includes 94 prefecture-level administrative units in eight provinces (89°20′–126°04′E, 31°23′–53°23′N), accounting for approximately 27.7% of the country's land area and 25% of its population (Xiao et al., 2021). As such, it provides an excellent research area with a large population, diverse economic development, vast landforms, and diverse cultivated land areas. Moreover, the YRB's terrain is high in the west and low in the east, spanning all three terrain types of China. The landforms are primarily divided into the Qinghai–Tibet Plateau, Inner Mongolia Plateau, Loess Plateau, and Huang-Huai-Hai Plain. Meanwhile, it also has a natural ecological corridor, namely the Yellow River, as well as several important ecological functional areas, including Sanjiangyuan, Qilian Mountain, and Zoige (Wu et al., 2013). The YRB also serves as an important ecological security barrier in China (Chen et al., 2021a, b, c; Liu et al., 2021), as well as an important region for population activities and economic development. Hence, the YRB has become a hot zone for studying the influence of human activities on the natural environment. Furthermore, in 2017, the cultivated land area was 3.694×10^5 km², with the grain production accounting for 29.5% of the country's total output (Liu et al., 2021). The per capita income of rural residents was 12,689 yuan in 2017. The YRB can provide useful lessons on how to alleviate hunger and poverty and ensure food security in regions and countries with little cultivated land (Fig. 1).

Data sources

The data included in this study comprise cultivated land data and socioeconomic data from eight provinces, derived from two sources. That is, Gansu, Henan, Qinghai, Shandong, and Shaanxi data were derived from their provincial statistical yearbooks in 2005, 2010, and 2017 (<https://navi.cnki.net/knavi/#>), whereas the data for Inner Mongolia, Ningxia, and Shanxi were derived from the China City Statistical Yearbook in 2005, 2010, and 2017 (<https://www.epsnet.com.cn/index.html#/Home>). Elevation raster data were obtained from the Chinese Academy of Sciences Resources Environmental Science Data Center Web site (<http://www.resdc.cn/Default.aspx>).

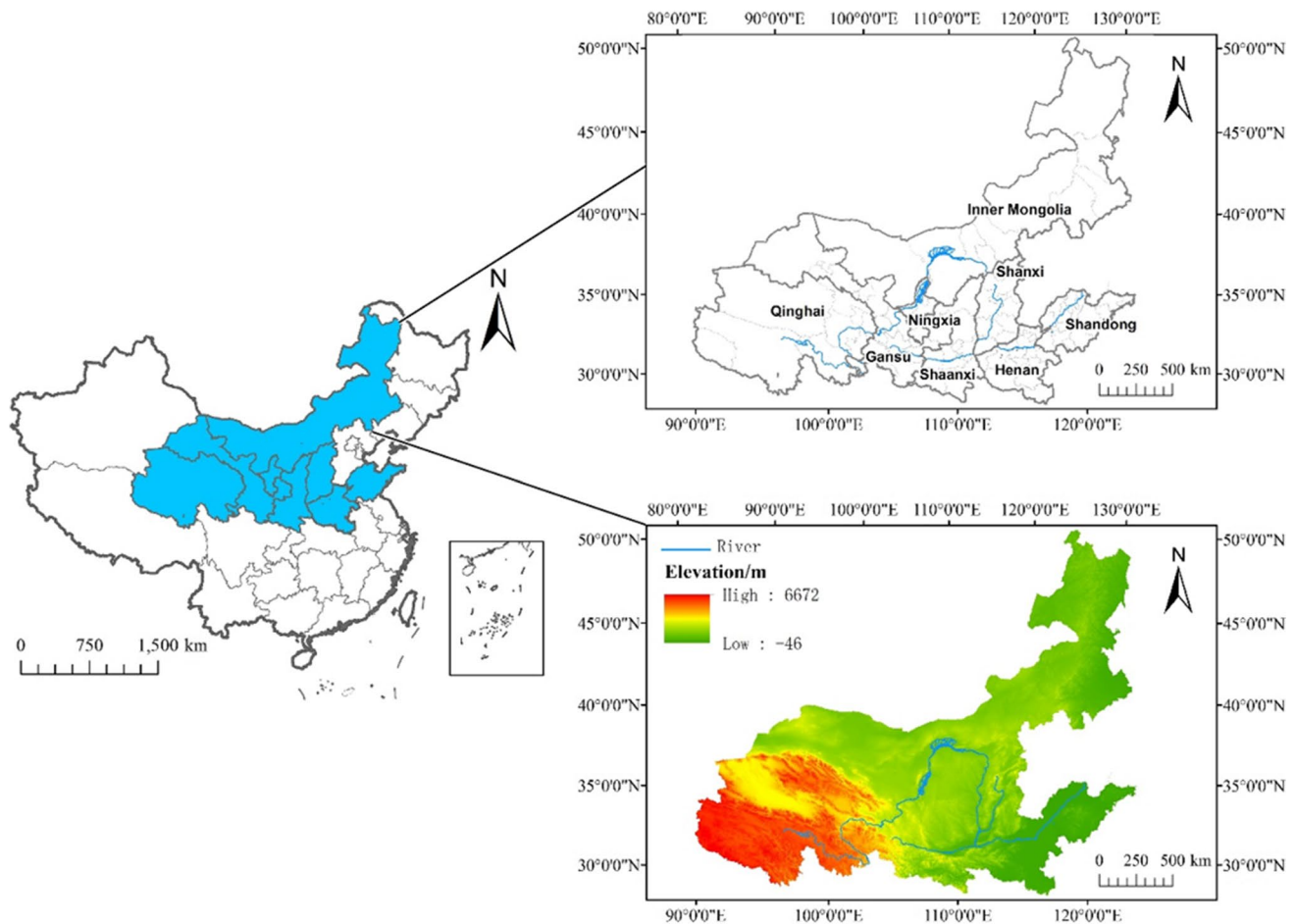


Fig. 1 Location of the Yellow River Basin in China

Methodology

We first adopted the comprehensive evaluation model and IPCC coefficient methodology to quantify the CLIU and CLCE of prefectural-level administrative units in the YRB in 2005, 2010, and 2017 and obtain their spatiotemporal evolution patterns. The carbon emission total efficiency (CETE), carbon emission pure technical efficiency (CEPTE), and carbon emission scale efficiency (CESE) of the YRB were then calculated for the corresponding years using the DEA-BCC model. Finally, bivariate spatial autocorrelation models were conducted to obtain the spatial correlation between CLIU and CETE, CLIU and CEPTE, as well as between CLIU and CESE in the corresponding years. The analytical framework used in this study is shown in Fig. 2.

Cultivated land intensive use

Selection of cultivated land intensive use indexes

In combination with previous studies (Ge et al., 2018; Liu et al., 2016; Zhou et al., 2013) and based on data

accessibility, this paper selected eleven indexes from three dimensions—input intensity, utilization degree, and output effect—to construct the evaluation index system of CLIU in the YRB. Input intensity is the basis of CLIU (Fan et al., 2012) and includes labor input per unit area, power input per unit area, fertilizer input per unit area, and farming financial input per unit area (Liu et al., 2016; Lou et al., 2017; Vallejo et al., 2015; Zhou et al., 2013). Hence, we selected the population of agricultural employment/cultivated land area, total power of agricultural machinery/cultivated land area, amount of chemical fertilizer/cultivated land area, and farming financial expenditures/cultivated land area to represent each of these inputs.

Utilization degree can reflect the state of CLIU (Liang and Li, 2020), which includes multiple cropping indexes, per capita cultivated land area, and per capita grain (Jaafar and Ahmad, 2020; Liu et al., 2016; Qi et al., 2020). As such, we selected total area used for sowing agricultural crops/cultivated land area, cultivated land area/total population, and total production of grain/total population to represent each utilization degree.

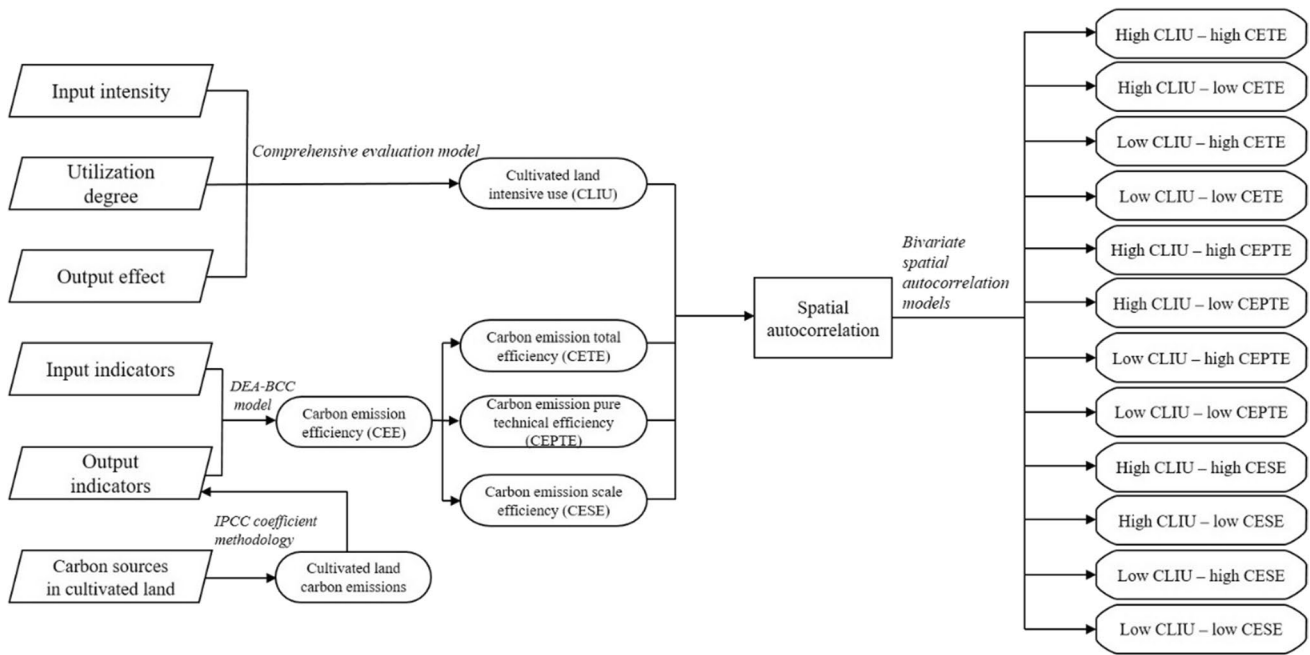


Fig. 2 Analysis framework

Output effect can reflect the externalities and income of CLIU (Ge et al., 2018) and include agricultural output value per unit area, agricultural output value per unit of labor, grain yield per unit area, and grain yield per unit of labor (Blanda et al., 2015; Ge et al., 2018; Some et al., 2019; Tian et al., 2021). As such, we selected gross output value of agriculture industry/cultivated land area, gross output value of agriculture industry/population of agricultural employment, total production of grain/cultivated land area, and total production of grain/population of agricultural employment to represent each output effect. Table 1 describes all indexes used in the evaluation system.

Calculation of cultivated land intensive use

In this study, the entropy weight method was first adopted to determine the weight of each index (Chen et al., 2018), after which the comprehensive evaluation model was adopted to measure CLIU (Huang et al., 2021). The CLIU in the YRB can be calculated using Eq. (1):

$$F_j = \sum_{i=1}^n \omega_i \times I_{ij} \tag{1}$$

where F_j is the comprehensive score value of CLIU in the j th evaluation unit, ω_i is the weight of the i th index, I_{ij} is the value of the i th index of the j th evaluation unit after standardized treatment, n is the number of evaluation indexes, and i is the evaluation index. Through Eq. (1), we obtained the results of the CLIU values in the YRB in 2005, 2010, and 2017.

Cultivated land carbon emissions

To calculate the CLCE in the YRB, we identified its major sources. Combined with the availability of data, we measured the CLCE in the YRB in 2005, 2010, and 2017 from four aspects: fertilizer, tillage, total area used for sowing agricultural crops, and total power of agricultural machinery (Table 2). Although this system only considers the cultivated land carbon sources in the YRB, it magnifies the actual CLCE to some extent, while reflecting the role of the carbon source in the cultivated land in the YRB. The CLCE in the YRB can be calculated using Eq. (2):

$$E = \sum_{i=1}^2 E_i + F = \sum_{i=1}^2 T_i \times \partial_i + (A \times B + C \times D) \tag{2}$$

where E represents the carbon emissions from cultivated land (kg), E_i represents the carbon emissions from fertilizers and plowing, F represents the carbon emissions from the production and use of agricultural machinery (unit kg), T_1 and T_2 are the amount of fertilizer and tillage carbon sources in kg and hm^2 , respectively, ∂_i is the carbon source coefficient, A is the total area used for sowing agricultural crops (in hm^2), C is the total power of the agricultural machinery (in kW), and B and D are the carbon emission coefficients of agricultural machinery.

Table 1 Description and weight of each evaluation index for cultivated land intensive use in the Yellow River Basin

Target layer	Criterion layer	Index layer	Effect	Index description	Weights	Reference
CLIU	Input intensity	Labor input per unit area	+	Population of agricultural employment/cultivated land area	0.0806	(Liu et al., 2016; Zhou et al., 2013)
		Power input per unit area	+	Total power of agricultural machinery/cultivated land area	0.0946	(May and Kocabiyik, 2019; Zhou et al., 2013)
		Fertilizer input per unit area	+	Amount of chemical fertilizer/cultivated land area	0.0868	(Doddabasawa et al., 2020; Lou et al., 2017)
		Farming financial input per unit area	+	Farming financial expenditures/cultivated land area	0.0408	(Lou et al., 2017; Vallejo et al., 2015)
	Utilization degree	Multiple cropping index	+	Total area used for sowing agricultural crops/cultivated land area	0.1147	(Briglia et al., 2019; Liu et al., 2016)
		Per capita cultivated land area	+	Cultivated land area/total population	0.0922	(Jaafar and Ahmad, 2020; Wu et al., 2019)
		Per capita grain	+	Total production of grain/total population	0.1028	(Qi et al., 2020; Zhou et al., 2013)
	Output effect	Agricultural output value per unit area	+	Gross output value of agriculture industry/cultivated land area	0.0899	(Liao et al., 2020; Some et al., 2019)
		Agricultural output value per unit of labor	+	Gross output value of agriculture industry/population of agricultural employment	0.0948	(Blanda et al., 2015; Dahal et al., 2020)
		Grain yield per unit area	+	Total production of grain/cultivated land area	0.0980	(Fan et al., 2012; Tian et al., 2021)
		Grain yield per unit of labor	+	Total production of grain/population of agricultural employment	0.1050	(Ge et al., 2018; Zhou et al., 2013)

Table 2 Carbon emission coefficients of carbon sources in the cultivated land

Carbon sources in cultivated land	Unit	Coefficient	Reference
Fertilizer	$kg \cdot kg^{-1}$	0.8965	(Garnier et al., 2019)
Tillage	$kg \cdot km^{-2}$	312.6	(Faust et al., 2019)
Total area used for sowing agricultural crops	$kg \cdot hm^{-2}$	16.47	(Gonzalez-Sanchez et al., 2012)
Total power of agricultural machinery	$kg \cdot kW^{-1}$	0.18	(Xia et al., 2017)

Carbon emission efficiency

Selection of carbon emission efficiency indexes

To simplify the calculation process and link to the CLIU index, this study constructed the cultivated land CEE index in the YRB from two input and output dimensions (Alamdarlo, 2018; Coderoni and Esposti, 2018; Paramesh et al., 2018; Zhu et al., 2018). When constructing the input indexes, we used the farming financial input per unit area and labor input per unit area to represent the inputs from the macroscopic perspective of capital and labor, respectively. When constructing the output indexes, CLCE should be

considered as a cost to better fit with the current low-carbon agricultural transition. Therefore, agricultural output value per unit of carbon emissions and grain yield per unit of carbon emissions were determined. Moreover, all price-related indexes had been converted to fixed prices based on the year 2005 (Table 3).

Calculation of carbon emission efficiency

Based on the multi-functional characteristics of cultivated land use in the YRB, the calculation model of CEE in the YRB was constructed using the DEA method, which has

Table 3 Input–output indexes of carbon emission efficiency for cultivated land use in the Yellow River Basin

Criterion layer	Index layer	Index description	Unit	Reference
Input indexes	Farming financial input per unit area	Farming financial expenditures/cultivated land area	$10^4 \text{ yuan}\cdot\text{km}^{-2}$	(Coderoni and Esposti, 2018; Paramesh et al., 2018)
	Labor input per unit area	Population of agricultural employment/cultivated land area	$10^4 \text{ person}\cdot\text{km}^{-2}$	(Dissanayake et al., 2020; Paramesh et al., 2018)
Output indexes	Agricultural output value per unit of carbon emissions	Gross output value of agriculture industry/cultivated land carbon emissions	$10^4 \text{ yuan}\cdot\text{t}^{-1}$	(Alamdarlo, 2018; Dong et al., 2017)
	Grain yield per unit of carbon emissions	Total production of grain/cultivated land carbon emissions	$\text{t}\cdot\text{t}^{-1}$	(Clark and Tilman, 2017; Zhu et al., 2018)

the advantage of analyzing the relative efficiency under multiple inputs and outputs (Chen et al., 2016; Yang et al., 2020). Currently, commonly used DEA models include the Charnes, Cooper, and Rhodes (CCR) model and the BCC model. The CCR model is an idealized input–output state, with an equal ratio of increasing inputs to outputs, which does not conform to the actual production situation, whereas the BCC model considers the increasing or decreasing marginal benefit, which more accurately reflects the true situation in the YRB (Clark and Tilman, 2017; Dong et al., 2017). The CEE in the YRB can be calculated using Eq. (3):

$$\begin{cases} \min [\theta - \varepsilon(e^{-T}s^- + e^T s^+)] \\ \sum_{j=1}^n X_j \lambda_j + s^- = \theta X_0 \\ \sum_{j=1}^n Y_j \lambda_j - s^+ = Y_0 \\ \sum_{j=1}^n \lambda_j = 1 \\ \lambda_j \geq 0, j = 1, 2, \dots, n, s^+ \geq 0, s^- \geq 0 \end{cases} \quad (3)$$

where X_j and Y_j are the input and output element sets of the decision-making units DMU_j , respectively; λ_j represents the combination proportion of the j th decision-making units when an effective DMU_0 is constructed through the existing combination; θ represents the effective value of the decision-making units DMU_0 , that is, the effective utilization degree of inputs and outputs. As θ approaches 1, the efficiency becomes more reasonable. ω is a non-Archimedes infinitesimal, and s^+ and s^- are relaxation variables, representing input redundancy and output deficiency, respectively.

In the BCC model, the total efficiency is the product of pure technical efficiency and scale efficiency; the calculation methods of CEPTE and CESE have been detailed previously (Khoshnevisan et al., 2013; Liou and Wu, 2011). An efficiency of one represents DEA effectiveness; otherwise, it represents invalid or weak effectiveness; the closer the value

is to one, the higher the efficiency. In our study, the CEPTE reflects whether the resource allocation of each decision-making unit is in an effective state in the process of CLIU, that is, the allocation and utilization efficiency of cultivated land resources in each area. CESE reflects the difference between the actual scale of the decision-making units and the optimal production scale, that is, the minimum input required to reach the existing output standard of unit carbon emissions. CETE is the product of CEPTE and CESE, which can reflect the capacity of regional cultivated land resource allocation, utilization, and scale aggregation, namely the efficiency of CLIU inputs to achieve the outputs per unit carbon emissions.

Spatial autocorrelation between cultivated land intensive use and carbon emission efficiency

Spatial autocorrelation analysis is a method of exploratory spatial data analysis, which is typically applied from three aspects. The first reveals geographical phenomena or attributes on a regional unit. The second reveals the degree of spatial correlation of the same phenomenon or attribute on adjacent regional units. The third measures the degree of spatial aggregation; this includes global spatial autocorrelation and local spatial autocorrelation (Zhang et al., 2021a, b, c).

Global spatial autocorrelation is used to describe the average correlation degree, spatial distribution pattern, and significance of all objects in the entire study area (Rodriguez-Galiano et al., 2012). Local spatial autocorrelation can identify the possible spatial correlation patterns in different spatial locations to determine the spatial local instability, grasp the aggregation and differentiation characteristics of local spatial elements more accurately, and provide a basis for classification and decision-making (Pratt and Chang, 2012). Generally, global Moran’s I and local Moran’s I indices are used to describe global spatial autocorrelation and local spatial autocorrelation, respectively. The global Moran’s I value can be calculated using Eq. (4), whereas the local Moran’s I value for a single spatial unit i is shown in Eq. (5):

$$I = \frac{\sum_{i=1}^n \sum_{j \neq i}^n W_{ij} \cdot (Y_i - \bar{Y}) \cdot (Y_j - \bar{Y})}{S^2 \cdot \sum_{i=1}^n \sum_{j \neq i}^n W_{ij}} \quad (4)$$

$$I_i = \frac{Y_i - \bar{Y}}{S_i^2} \cdot \sum_{i=1, j \neq i}^n W_{ij} \cdot (Y_i - \bar{Y}) \quad (5)$$

where $S^2 = \frac{1}{n} \sum_{i=1}^n (Y_i - \bar{Y})^2$, $\bar{Y} = \frac{1}{n} \sum_{i=1}^n Y_i$; Y_i and Y_j represent attribute values of units i and j , respectively; n is the total number of evaluated areas; and W_{ij} is a weight matrix based on the spatial adjacency relationship.

To describe the spatial correlation among multiple variables, the bivariate global autocorrelation and local autocorrelation have been expanded based on the Moran's I index, providing a feasible method for defining the spatial correlation in the distribution of different elements (Zhou et al., 2020). See Eq. (6) for details.

$$I_{lm}^p = z_l^p \cdot \sum_{q=1}^n W_{pq} \cdot z_m^q \quad (6)$$

where $z_l^p = \frac{X_l^p - \bar{X}_l}{\sigma_l}$, $z_m^q = \frac{X_m^q - \bar{X}_m}{\sigma_m}$; X_l^p is the value of attribute l of spatial unit p ; X_m^q is the value of attribute m of spatial unit q ; \bar{X}_l and \bar{X}_m are the mean values of attributes l and m , respectively; σ_l and σ_m are the variances of attributes l and m , respectively; and W_{pq} is the spatial connection matrix between spatial units p and q .

Results

Spatiotemporal patterns of cultivated land intensive use in the Yellow River Basin

In 2005, 2010, and 2017, the number of cities with CLIU > 0.251 was 12, 37, and 46, respectively, thus representing a gradual upward trend with time. Higher CLIU areas were predominantly distributed in the southeast of the YRB (mainly Shandong and Henan provinces) and were largely associated with their location in the North China Plain, an area with a developed economy, perfect agricultural infrastructure, and high levels of agricultural mechanization. Other higher CLIU areas included northeastern and northwestern Inner Mongolia, northwestern Gansu, northern Ningxia, and southern Shaanxi. Among them, higher CLIU areas were relatively concentrated in the northwest of the YRB (Fig. 3), which was attributed to socioeconomic development and the application of new and advanced technology.

Spatiotemporal patterns of cultivated land carbon emissions in the Yellow River Basin

The total CLCE values in the YRB in 2005, 2010, and 2017 were 2.892×10^7 t, 3.662×10^7 t, and 3.671×10^7 t, respectively, indicating a continuous increase with time. High CLCE areas were primarily concentrated in the Shandong Peninsula agglomeration and the Central Plains agglomeration (Fig. 4), which was largely attributed to China's Agricultural Mechanization Promotion Law and implementation of fertile soil projects. Low CLCE areas were found to be primarily concentrated in the western, northern, and central areas of the YRB, including Qinghai, Gansu, Ningxia, Shaanxi, and Shanxi provinces, as well as central and western Inner Mongolia, which was largely attributed to the Grain for Green policy and the "Sunshine Project" for rural labor transfer.

Spatiotemporal patterns of carbon emission efficiency in the Yellow River Basin

Spatiotemporal patterns of carbon emission total efficiency

The average CETE values in the YRB in 2005, 2010, and 2017 were 0.408, 0.324, and 0.356, respectively, which were relatively low and exhibited an initial decrease followed by a slight increase. The proportion of cities with CETE values exceeding 0.501 during 2005, 2010, and 2017 was 36.17%, 15.96%, and 22.34%, respectively. Importantly, the CETE in the YRB was in a general period of adjustment during the study period. Higher CETE areas were predominantly distributed in the northeast of Inner Mongolia, Shandong Peninsula agglomeration, Central Plains agglomeration, Shaanxi Province, and northwest Gansu Province. The fact that cities with rapid economic development in the YRB commonly have a high input of cultivated land use and high-carbon dioxide emissions explains why cities with higher CETE values were primarily located in rapidly developing economic areas. Specifically, the strategy adopted by the eastern coastal area of taking the lead in development led to an inflow of economic production elements, such as labor and capital, to coastal areas. The rebalance between coastal and inland area strategies promoted the rapid rise of agglomerations in the central and western areas. Thus, higher CETE areas appeared predominantly in eastern areas, followed by central and western cities (Fig. 5a1–a3).

Spatiotemporal patterns of carbon emission pure technical efficiency

The average CEPTE values in 2005, 2010, and 2017 were 0.651, 0.630, and 0.615, respectively, which were relatively

Fig. 3 Spatiotemporal evolution of cultivated land intensive use in the Yellow River Basin from 2005 to 2017

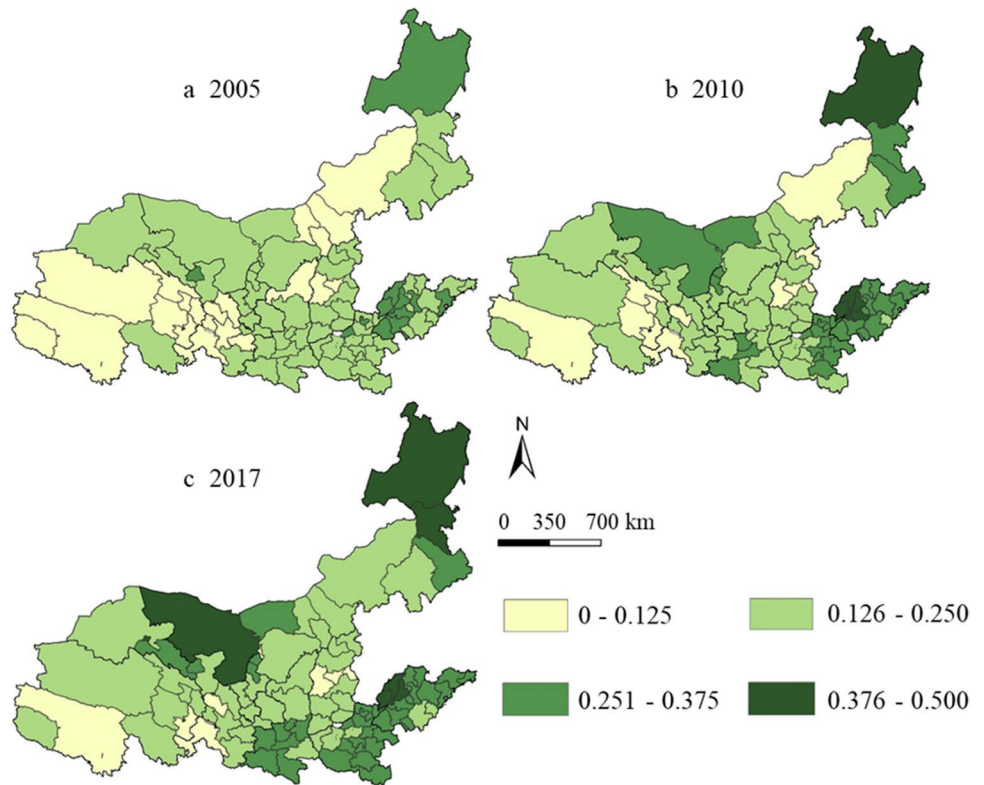
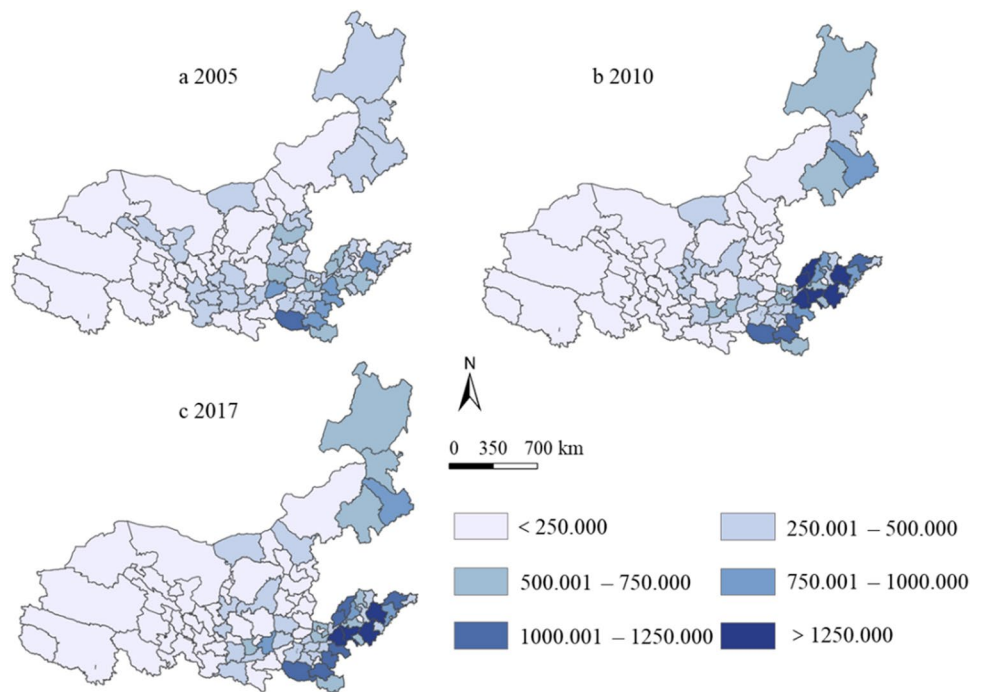


Fig. 4 Spatiotemporal evolution of cultivated land carbon emissions in the Yellow River Basin from 2005 to 2017



high and showed a gradual decreasing trend. The number of cities in the range of 0.501–0.999 was 51.06% in 2005, 62.77% in 2010, and 54.26% in 2017. The higher CETE areas were primarily distributed in Shandong,

Henan, Shanxi, Inner Mongolia, Gansu, southern Shaanxi, and southern Qinghai provinces (Fig. 5b1–b3). This was largely due to the southeast coastal cities having entered the advanced stage of cultivated land use by this time, with

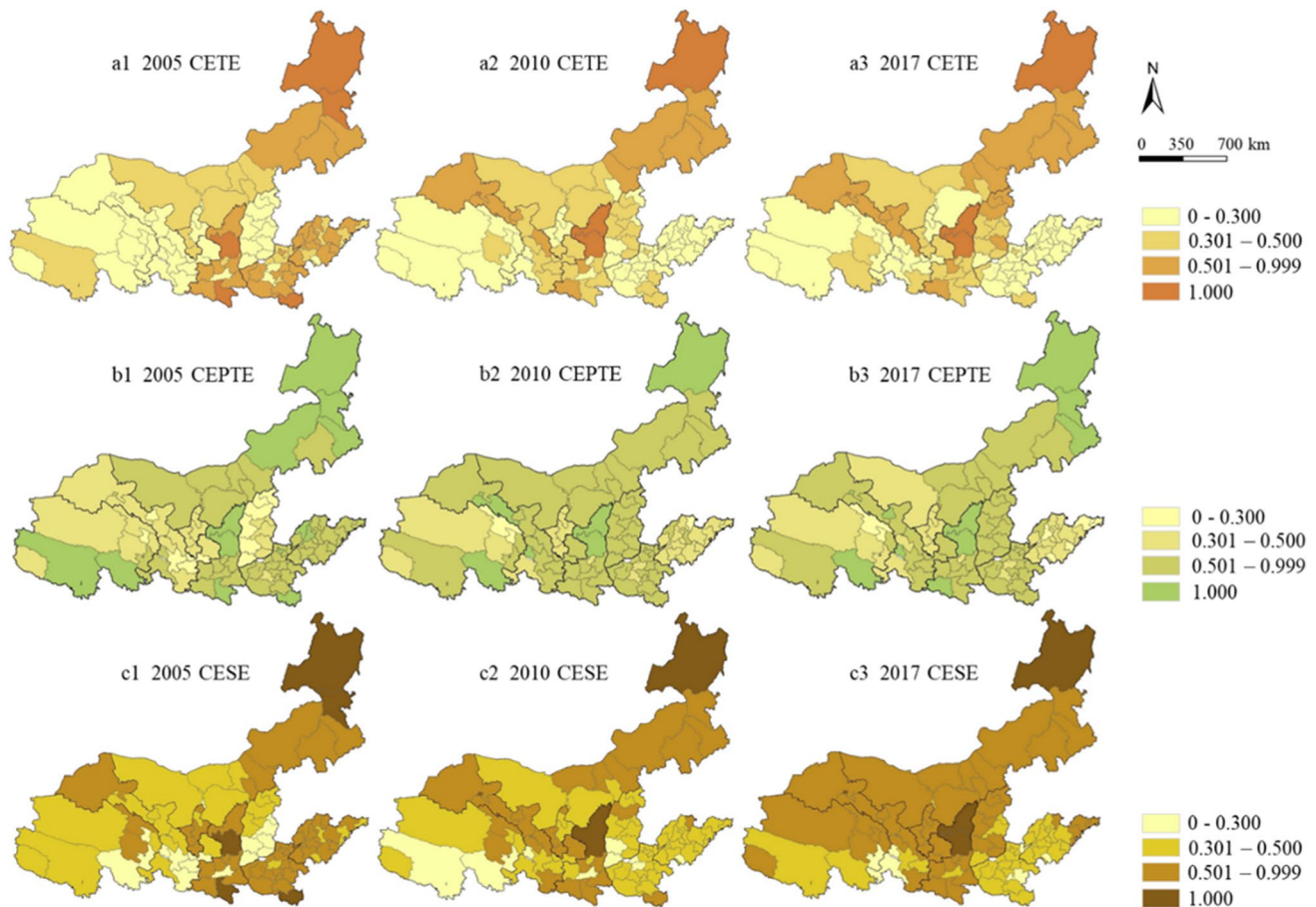


Fig. 5 Spatiotemporal evolution of three carbon emission efficiency types in the Yellow River Basin from 2005 to 2017. CETE, carbon emission total efficiency; CEPTE, carbon emission pure technical efficiency; CESE, carbon emission scale efficiency

intelligent mechanization representing the dominant cultivated land use mode. During the same period, cultivated land use in the other areas entered the transition development period in response to the YRB high-quality development strategy.

Spatiotemporal patterns of carbon emission scale efficiency

The average CESE values of the YRB in 2005, 2010, and 2017 were 0.574, 0.503, and 0.560, respectively. The average values were relatively high, exhibiting an initial decrease and subsequent increase. During the study period, although the CESE and CETE spatial distributions in the YRB were similar they exhibited differences, which were reflected by their relative proportions within the range of 0.501–0.999. The CESE proportions in 2005, 2010, and 2017 were 50.00%, 29.79%, and 51.06%, respectively, which were higher than those of CETE in the same period. This indicated that the CESE in the YRB was in a transitional period. Higher CESE areas were primarily distributed in the Shandong Peninsula

agglomeration, Central Plains agglomeration, Guanzhong agglomeration, Taiyuan agglomeration, Hohhot–Baotou–Ordos–Yulin agglomeration, Lanzhou–Xining agglomeration, and the Ningxia agglomerations of the Yellow River. The ecological civilization construction strategy, together with the development of green agriculture strategies, was the primary cause if the CESE values increase in these areas. Other areas with high CESE included Inner Mongolia and the northern areas of Qinghai Province (Fig. 5c1–c3).

Spatial autocorrelation analysis in the Yellow River Basin

Global spatial autocorrelation analysis of cultivated land intensive use and carbon emission efficiency in the Yellow River Basin

The Moran scatter plot reflects the spatial correlations between CLIU and lagged CETE, CLIU and lagged CEPTE, and CLIU and lagged CESE in the YRB, which

can be divided into four quadrants. Among them, the first quadrant (high–high (HH) clustering type) and the third quadrant (low–low (LL) clustering type) showed positive spatial correlations between CLIU and lagged CETE, CLIU and lagged CEPTE, and CLIU and lagged CESE. Additionally, the second quadrant (low–high (LH) outlier type) and the fourth quadrant (high–low (HL) outlier type) showed negative spatial correlations between CLIU and lagged CETE, CLIU and lagged CEPTE, and CLIU and lagged CESE (Fig. 6).

The results from the global bivariate Moran’s I values revealed a significant positive spatial autocorrelation between CLIU and all three types of CEE in 2005 (all Moran’s I values > 0 and $p = 0.001$), indicating that the increase in CLIU led to an increase in all three types of CEE in the YRB in 2005. The positive autocorrelation between CLIU and CEPTE (Moran’s I : 0.3849) was the strongest, followed by that between CLIU and CETE (Moran’s I : 0.3667) and between CLIU and CESE (Moran’s I : 0.2920). Moreover, a significant negative spatial autocorrelation

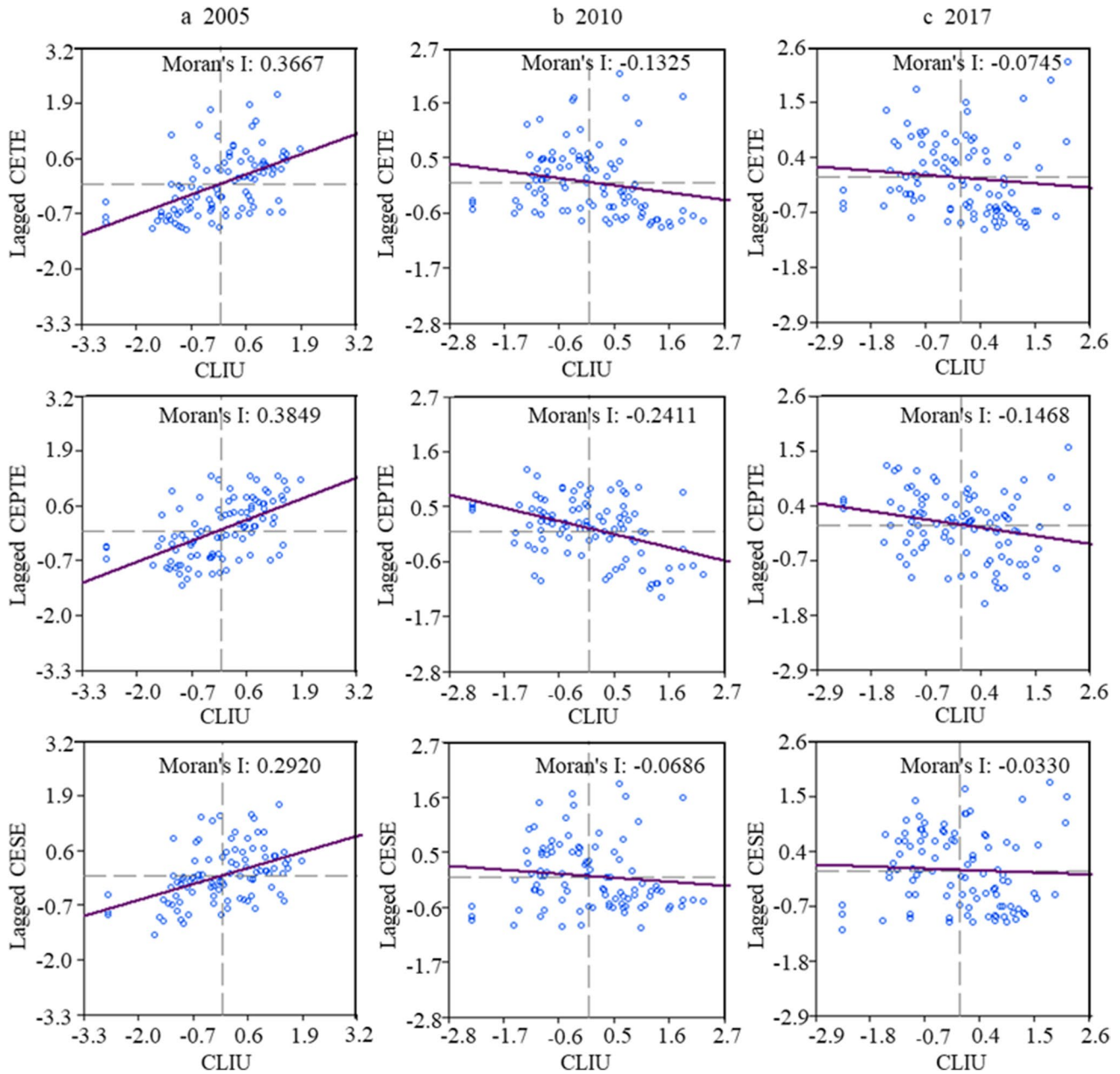


Fig. 6 Moran scatter plot between cultivated land intensive use and three types of carbon emission efficiency in the Yellow River Basin from 2005 to 2017. CLIU, cultivated land intensive use; CETE, car-

bon emission total efficiency; CESE, carbon emission scale efficiency; CEPTE, carbon emission pure technical efficiency

was detected between CLIU and all three types of CEE in 2010 (all Moran's I values < 0), indicating that an increase in CLIU in the YRB led to a decrease in the three types of CEE in 2010. CLIU and CEPTE (Moran's I : -0.2411 , $p=0.001$) had the strongest negative correlation, followed by CLIU and CETE (Moran's I : -0.1325 , $p=0.006$). Meanwhile, the negative correlation between CLIU and CESE (Moran's I : -0.0686 , $p=0.089$) was the weakest. In 2017, CLIU was negatively correlated with all three CEE types. CLIU and CEPTE exhibited the strongest negative correlation (Moran's I : -0.1468 , $p=0.003$), followed by CLIU and CETE (Moran's I : -0.0745 , $p=0.059$) then CLIU and CESE (Moran's I : -0.0330 , $p=0.256$).

Moreover, the absolute values for Moran's I values between CLIU and all three types of CEE during 2005 to 2017 all decreased from largest to smallest. Hence, the aggregation degree between CLIU and all three types of CEE decreases with time, while the dispersion degree increases with time, and the spatial correlation weakens gradually.

Local spatial autocorrelation analysis of cultivated land intensive use and carbon emission efficiency in the Yellow River Basin

According to the bivariate local indicators of spatial autocorrelation cluster maps, CLIU and the three types of CEE exhibited four types of spatial autocorrelation in 2005, 2010, and 2017 (Fig. 7). From the perspective of time, the number of HL and LH clusters gradually increased, whereas the number of HH and LL clusters gradually decreased. Moreover, the number of HL and LL clusters showed a significant difference between 2005 and 2010. That is, in 2005, the results of local spatial autocorrelation showed that CLIU and the three types of CEE in the YRB were dominated by HH and LL clusters. HH clusters were mainly distributed in the northeast and southeast of the YRB and were concentrated in the northeast of Inner Mongolia, Shandong Peninsula agglomeration, and south of Central Plains agglomeration, whereas LL clusters were primarily distributed in the west of the YRB and were concentrated in the Ningxia agglomerations of the Yellow River and the Lanzhou–Xining agglomeration (Fig. 7a1, b1, c1). In contrast, in 2010, HL and LH were the dominant clusters for CLIU and CETE, with HL clusters primarily distributed in the southeast of the YRB, and concentrated in the Shandong Peninsula agglomeration. Meanwhile, the LH clusters were more dispersed, primarily in the northeast of Inner Mongolia and the Taiyuan agglomeration (Fig. 7a2, b2).

The CLIU and CESE clusters exhibited obvious spatial heterogeneity (Fig. 7c2). In 2017, both CLIU and the three types of CEE in the YRB were dominated by HL and LH clusters. HL clusters were primarily distributed in the

southeast of the YRB and concentrated in the Shandong Peninsula agglomeration, whereas LH clusters were distributed primarily in the northeast and central areas of the YRB and concentrated in the northeast of Inner Mongolia, as well as the Taiyuan agglomeration, Hohhot–Baotou–Ordos–Yulin agglomeration, and Ningxia agglomerations of the Yellow River (Fig. 7a3, b3, c3). Moreover, nonsignificant areas in Fig. 7 were largely concentrated in the central and western regions of the YRB.

Discussion

Impacts of cultivated land intensive use on carbon emission efficiency

Overall, the CLIU and CLCE values in the YRB exhibited a continuously increasing trend, while areas with higher CLCE were concentrated in the southeast of the YRB. These findings are supported by those of previous studies over the past two decades related to various policies and laws, such as the comprehensive implementation of the project to return cultivated land to forests, the promotion of China's Agricultural Mechanization Promotion Law, the launch of fertile soil projects, and the rebalance of cultivated land occupation and replenishment (Cheng et al., 2017; Li et al., 2020; Li et al., 2019a, b; Zhang et al., 2020).

Initially, land intensive use became popular to ensure food security and promote agricultural modernization. Consequently, North China has developed a large number of domestic and foreign industries with high-carbon emissions (Zhao and Yin, 2011). For example, chemical fertilizers, agricultural machinery, and pesticides are widely used in agricultural production (Chen and Xie, 2019). However, the rapid urban expansion over the past two decades has resulted in a significant loss of high-quality cultivated land (Xiao et al., 2021), as well as the use of many high-carbon emission factors (Wang et al., 2018a, b). Among them, agriculture and urbanization in the Huang-Huai-Hai Plain were the fastest to develop in the YRB (Shi et al., 2013), and its CLCE was much higher than that of other regions of the YRB. Specifically, within this region, the average CETE and CESE values were found to first decrease from 2005 to 2010 and subsequently increase by 2017, whereas the average CEPTE values exhibited a continual gradual decrease. Alternatively, areas of higher CETE, CESE, and CEPTE were predominantly found in eastern areas, followed by central and western areas of the YRB. Similar findings have been previously reported when investigating the east and west rebalance in the Chinese strategy (Fukumoto and Muto, 2012), the Made in China 2025 strategy (Wang et al., 2020), and the high-quality development strategy (Chen et al., 2020a, b, c), all of which have supported the upgrade

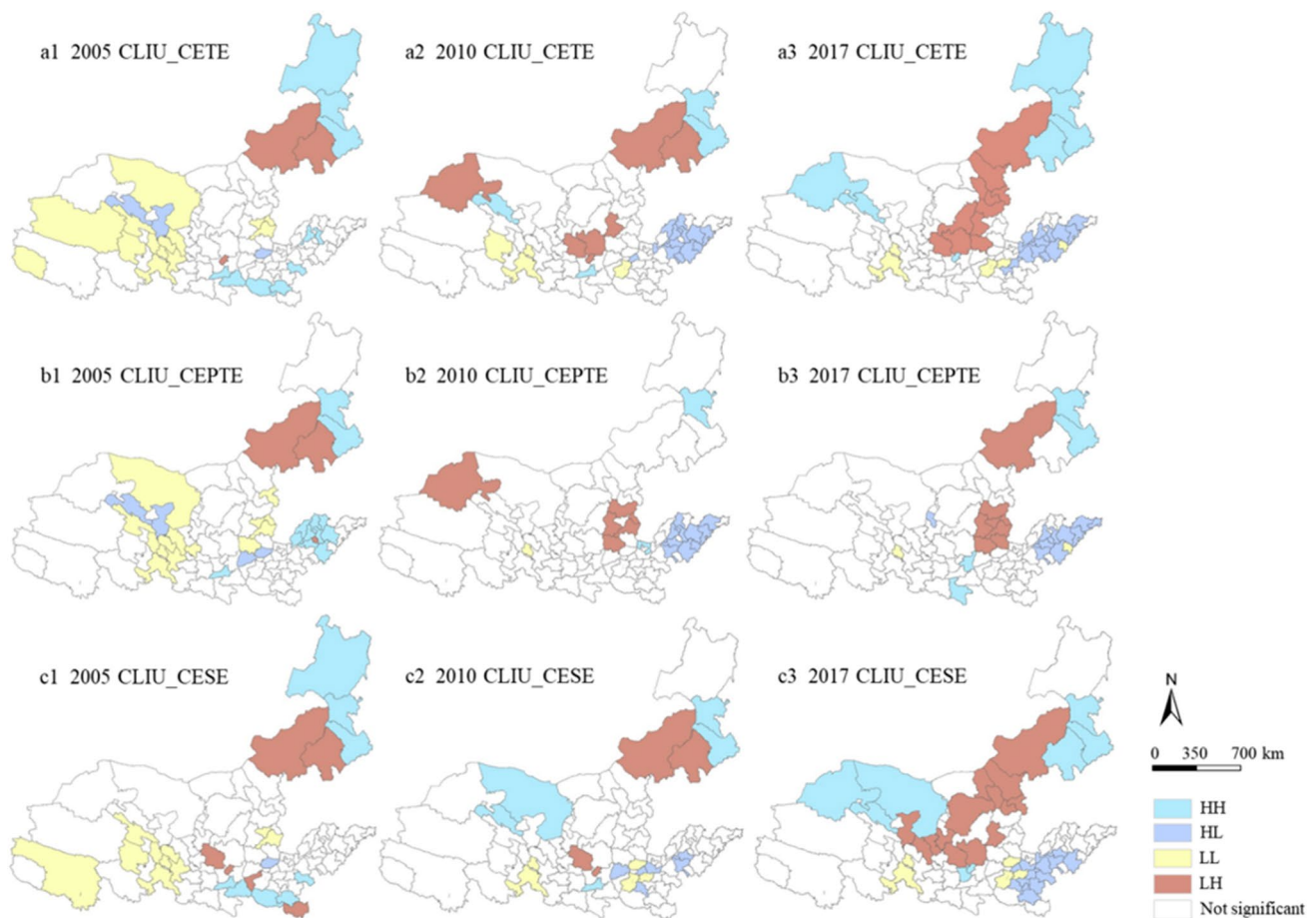


Fig. 7 Local indicators of spatial autocorrelation cluster maps between cultivated land intensive use and three types of carbon emission efficiency in the Yellow River Basin from 2005 to 2017. a1 to a3 represent local bivariate spatial autocorrelations between cultivated land intensive use and carbon emission total efficiency from 2005 to 2017; HH, high cultivated land intensive use and high-carbon emission total efficiency cluster; HL, high cultivated land intensive use

and low-carbon emission total efficiency cluster; LH, low cultivated land intensive use and high-carbon emission total efficiency cluster; LL, low cultivated land intensive use and low-carbon emission total efficiency cluster; CLIU, cultivated land intensive use; CETE, carbon emission total efficiency; CESE, carbon emission scale efficiency; CEPTE, carbon emission pure technical efficiency

of local industries to technologically intensive strategies. Indeed, the central and western regions have undertaken various capital- and labor-intensive industries (Lemoine et al., 2015), effectively disrupting the balance between local original capital factors and labor factors, causing the CEE to change.

The global spatial autocorrelation analysis showed that CLIU and CEE have significant spatial dependence from positive correlations to negative correlations. The aggregation degree between CLIU and CEE gradually decreases with time, while the dispersion degree increases with time, and the spatial correlations gradually weaken. Additionally, the local spatial autocorrelation showed that the number of HL and LH clusters between CLIU and CEE gradually increased over time, while that of HH and LL clusters gradually decreased. Previous studies have shown that land intensive use negatively correlates

with carbon emissions (Xie et al., 2018) with no apparent spatial correlation or spatial spillover effect (Wang et al., 2019). This study confirms, and refines, these results. In general, CLIU has a negative spatial spillover effect on CEE; that is, an improved CLIU in one area may lead to a decrease in CEE within the surrounding areas. Those with a high CLIU, such as Shandong Peninsula agglomeration and Central Plains agglomeration, are CEE low-value regions, while those with low CLIU, such as Hohhot–Baotou–Ordos–Yulin agglomeration and Taiyuan agglomeration, are CEE high-value regions. This is because CEE is not only affected by capital and labor force but also by the comprehensive effects of economic policies, industrial structure, and technological level, among other factors (Pan et al., 2020; Yang et al., 2021; Zhang and Chen, 2021). In particular, under the more recent influence of policies implemented for western development (Song and

Zhou, 2021), as well as the industrial transfer within eastern coastal regions (Chuai et al., 2015), and the rise of the central region (Ding et al., 2021), the state has made a significant investment in developing infrastructure within the central and western regions, thus creating conditions for the large-scale migration of industrial capital and labor force. However, currently, the areas with higher CLCE values are concentrated in the southeast region of the YRB, causing a decline in the overall spatial aggregation degree between CLIU and CEE. Moreover, the LH clusters increased and expanded within the central region of the YRB, indicating that the core attractants, such as enterprise tax policy, population settlement policy, vocational education and training, medical and social security services, transportation and communication costs, in this area are more conducive to CEE than those of other regions within the YRB. This apparent preference for the central region has resulted from its taking the initiative to prepare for the aftereffects of the coastal and inland rebalancing strategy (Lemoine et al., 2015), the belt and road initiative (Wu et al., 2021), and the rural revitalization strategy (Liu et al., 2020a, b, c). That is, the central areas migrated relevant industries, established factories, provided sufficient employment opportunities, and promoted the return of labor force with the spillover effect of the Hohhot–Baotou–Ordos–Yulin agglomeration and Taiyuan agglomeration. Meanwhile, the HL clusters continued to increase in the southeast region of the YRB due to the disproportionate use of high-carbon emission elements in Shandong Peninsula agglomeration and Central Plains agglomeration compared to the other YRB regions (Wang et al., 2018a, b). Thus, to facilitate construction of an ecological civilization with green development, there is an increasing demand for industries to transform to low-carbon utilization with priority given to the development of a green economy.

The relationship between CLIU and CLCE may exist in multiple stages exhibiting an “inverted U shape” or fluctuation type. In this study, the CLIU increase did not reach the inflection point of the CLCE decrease. A change in CLCE serves as an early warning standard for CEE (Dong et al., 2020). Furthermore, the relationship between CLIU and CLCE is an important basis for cultivated land use strategy, cultivated land resource allocation adjustment, and cultivated land emission reduction policy formulation. Moreover, CLCE is the negative externality of the CEE system for cultivated land (Maraseni et al., 2021). Therefore, identifying the degree of interference made by CLCE on CEE is necessary for optimizing CLIU. A change in CLIU type may lead to drastic changes in the efficiency of cultivated land output per unit of carbon emissions, regional cultivated land resource allocation and utilization efficiency, and the minimum carbon emission input required to meet the

existing output standard per unit of carbon emissions (Ni et al., 2021). Therefore, constructing a virtuous cycle within the cultivated land use system and actively guiding CLIU to develop toward low-carbon output is an effective strategy to optimize and improve regional CEE.

Policy implications

To ensure food security and accelerate the green and low-carbon transition, cultivated land protection policies in the YRB should primarily protect high-quality cultivated land, particularly that in the main grain-producing areas (Wu et al., 2017). For example, policymakers in major grain-producing areas can set up a small-to-large compensation and reward matching mechanism (Matzek et al., 2020) to motivate enterprises, cooperatives, or individuals that meet carbon dioxide emission reduction targets to engage in low-carbon production. Moreover, due to long-term water shortages in the Loess Plateau, policymakers should prioritize high-efficiency water-saving irrigation technology to improve irrigation efficiency (Cremades et al., 2016). Administrative departments may also provide online reputation recognition for enterprises or individuals who improve, apply, or promote new technologies or patents. Furthermore, the government should encourage enterprises and scientific research institutions to develop more environmentally friendly agricultural additives (Li et al., 2019a, b), control agricultural non-point source pollution, and protect the fragile plateau.

Due to rapid urbanization in the YRB, the agricultural population is becoming non-agricultural (Chen et al., 2019; Xie and Liu, 2015). To replace the agricultural population and ensure food security, policies regarding the regulation and control of cultivated land use were previously implemented to account for the impact of labor shortages on agricultural development (Lu et al., 2019). These measures indirectly led to an increase in the use of chemical fertilizers, pesticides, electricity, fossil energy, and other products, as well as an increase in carbon emissions (Li et al., 2021a, b), resulting in an agricultural ecological imbalance. In recent years, the rapid development of transportation infrastructure in the YRB, especially expressways and high-speed railways (Chen et al., 2020a), has accelerated the flow of labor, technology, and capital. This has created convenient conditions for the coordinated development of agriculture in the eastern and western areas of the YRB. Therefore, to achieve carbon neutrality coordination and joint efforts must be made between surrounding areas, as well as stronger cooperation between all levels of government to ensure the transition of existing arable land use toward low-carbon and high-efficiency land use.

The YRB comprises eight provinces with different cultivated land conditions, resource endowments, and economic levels. In the future, it will be beneficial for the government

to create differentiated policies based on a comprehensive consideration of the cultivated land policies of different provinces, their specific technical effects, and their costs. For instance, in economically developed areas, emphasis should be placed on improving the quality of cultivated land, strengthening supervision, and reducing administrative intervention (Yan et al., 2020). Alternatively, in economically underdeveloped areas, emphasis should be placed on the ecological function of cultivated land, consolidating the basic position of agriculture, and promoting farmer employment (Yang et al., 2016). Meanwhile, for the main grain-producing areas, the emphasis should be on ensuring the amount of cultivated land and limiting the occupancy of cultivated land (Guo et al., 2021). Moreover, fiscal support for petroleum agriculture should be reformed in the eastern areas of the YRB, and subsidies for fertilizer production and consumption should be phased out (Liu et al., 2020a, b, c).

In the western areas of the YRB, financial institutions should be encouraged to provide farmers with more convenient agricultural financial services (Elahi et al., 2018). For example, the government has guided village collectives to integrate cultivated land resources and has invited planning companies to create cultivated land products based on local characteristics. As such, the ownership and rights to the use of cultivated land products produced by the integrated cultivated land belong to the village collective, for which they are regarded as ecological assets. Village collectives can mortgage their right to use in the form of creditor's rights to financial institutions, which issue specific financial derivatives or debts. The financial institutions should then regularly pay dividends to the village collectives according to the proportion agreed upon in the contract and provide more convenient and specific financial services for the villagers participating in the project. For example, low-interest study tour loans can be provided to villagers to allow them to travel to developed countries or regions for 90–180 days, thereby enriching their knowledge and promoting cultural exchange. Additionally, the expansion of construction land should be limited (Huang et al., 2019). For example, state-owned commercial banks should be encouraged to provide additional credit rating services to local law firms, who should then be encouraged to regularly provide public welfare legal services to farmers. This measure can improve the business scope of state-owned commercial banks, address legal and institutional loopholes, and expand the popularity and reputation of law firms. Mostly, the government should issue related policies to award priority to the land capital appreciation income and other related rights and interests of land-lost farmers in the future.

Limitations and future prospects

In this study, we measured the spatial correlation between CLIU and CEE in the YRB. However, other factors also

affect CEE, such as the cost of carbon dioxide emission reduction, the application of low-carbon technology in agriculture, and the degree of farmers' professionalism (Meijboom and Staffleu, 2016). These aspects were not measured in this study and, thus, require further analysis in future studies. Moreover, economic growth is a decisive factor in cultivated land use change (Zhou et al., 2020); therefore, when evaluating CLIU in the YRB in the future, we will consider economic indicators, such as investment in irrigation renovation projects, investment in agricultural fixed assets, and the wages of hired workers in the harvest season.

Conclusion

In this study, we used a comprehensive evaluation model to quantify the spatiotemporal characteristics of CLIU in the YRB and measure CLCE by IPCC coefficient methodology. We then popularized a DEA model to identify the cultivated land CEE. Finally, a spatial autocorrelation method was used to test the spatial correlation between the CLIU and CEE. According to the results, the overall CLIU and CLCE values in the YRB exhibited a continuous increase; the average CETE and CESE first decreased and then increased, and the average CEPTE slowly decreased. Areas of high CLCE were concentrated in eastern regions of the YRB, whereas areas of high CLIU, CETE, CESE, and CEPTE predominantly appeared in the eastern areas, followed by central and western regions of the YRB. Spatial analysis revealed significant spatial dependence of CLIU on CEE. From a global perspective, there were positive and negative spatial correlations between CLIU and CEE, which changed from positive to negative with time. The aggregation degree between CLIU and CEE gradually decreased with time, the dispersion degree increased with time, and the spatial correlations gradually weakened. Locally, HL and LH clusters became gradually more dominant. Therefore, to facilitate future carbon emission reduction, relevant policies should not only coordinate the complex relationship between capital and labor, but also give priority to groups representing advanced technology and management skills. Finally, regions near the areas of high CEE should avoid negative environmental effects caused by spillover effects from urban sprawl and massive loss of cultivated land. As such, the area surrounding the lower CEE should be dedicated to eco-friendly land use.

Acknowledgements Not applicable.

Authors' contributions XZ and WC proposed conceptualization and methodology. XZ and JY collected and organized datasets. XZ, JY, DZ, DW, and SP ran models, analyzed the results, and visualized the study. XZ and WC wrote the original draft. JL, SL, and WC reviewed the manuscript. All authors read and approved the final manuscript.

Funding The research is sponsored in part by grants from the Natural Science Foundation of China (Grant No. 42001187 and 41971245).

Data Availability The datasets used and analyzed during the current study are available from the corresponding author upon request.

Declarations

Ethics approval and consent to participate Not applicable.

Consent for publication Not applicable.

Competing interests The authors declare no competing interests.

References

- Abe SS, Ashida K, Kamil MI, Tobisaka K, Kamarudin KN, Hermansah, Umami IM (2020) Land use and management effects on volcanic soils in West Sumatra Indonesia. *Geoderma Reg* 22:e00308
- Ahmad M, Muslija A, Satrovic E (2021) Does economic prosperity lead to environmental sustainability in developing economies? Environmental Kuznets curve theory. *Environ Sci Pollut Res* 28(18):22588–22601
- Akram R, Chen FZ, Khalid F, Huang GH, Irfan M (2021) Heterogeneous effects of energy efficiency and renewable energy on economic growth of BRICS countries: A fixed effect panel quantile regression analysis. *Energy*. 215:119019
- Alamdarlo HN (2018) The economic impact of agricultural pollutions in Iran, spatial distance function approach. *Sci Total Environ* 616:1656–1663
- Ameur F, Amichi H, Leauthaud C (2020) Agroecology in North African irrigated plains? Mapping promising practices and characterizing farmers' underlying logics. *Reg Environ Change* 20:133
- Arneth A, Sitch S, Pongratz J, Stocker BD, Ciais P, Poulter B, Bayer AD, Bondeau A, Calle L, Chini LP, Gasser T, Fader M, Friedlingstein P, Kato E, Li W, Lindeskog M, Nabel J, Pugh TAM, Robertson E, Viovy N, Yue C, Zaehle S (2017) Historical carbon dioxide emissions caused by land-use changes are possibly larger than assumed. *Nat Geosci* 10:79–86
- Bajan, B., Mrowczynska-Kaminska, A., 2020. Carbon footprint and environmental performance of agribusiness production in selected countries around the world. *J Clean Prod* 276.
- Blanda E, Drillet G, Huang CC, Hwang JS, Jakobsen HH, Rayner TA, Su HM, Wu CH, Hansen BW (2015) Trophic interactions and productivity of copepods as live feed from tropical Taiwanese outdoor aquaculture ponds. *Aquaculture* 445:11–32
- Briglia N, Petrozza A, Hoeberichts FA, Verhoef N, Povero G (2019) Investigating the Impact of Biostimulants on the Row Crops Corn and Soybean Using High-Efficiency Phenotyping and Next Generation Sequencing. *Agronomy-Basel* 9:761
- Chen JD, Cheng SL, Song ML (2017) Estimating policy pressure for China's cultivated land use protection based on an extended index. *Phys Chem Earth* 101:21–34
- Chen, Q.R., Xie, H.L., 2019. Temporal-Spatial Differentiation and Optimization Analysis of Cultivated Land Green Utilization Efficiency in China. *Land*. 8(11).
- Chen ST, Guo B, Zhang R, Zang WQ, Wei CX, Wu HW, Yang X, Zhen XY, Li X, Zhang DF, Han BM, Zhang HL (2021a) Quantitatively determine the dominant driving factors of the spatial-temporal changes of vegetation NPP in the Hengduan Mountain area during 2000–2015. *J Mt Sci-Engl* 18(2):427–445
- Chen W, Li H, Hou EK, Wang SQ, Wang GR, Panahi M, Li T, Peng T, Guo C, Niu C, Xiao LL, Wang JL, Xie XS, Bin Ahmad B (2018) GIS-based groundwater potential analysis using novel ensemble weights-of-evidence with logistic regression and functional tree models. *Sci Total Environ* 634:853–867
- Chen WX, Chi GQ, Li JF (2019) The spatial association of ecosystem services with land use and land cover change at the county level in China, 1995–2015. *Sci Total Environ* 669:459–470
- Chen WX, Chi GQ, Li JF (2020) The spatial aspect of ecosystem services balance and its determinants. *Land Use Policy* 90:104263
- Chen WX, Zhao HB, Li JF, Zhu LJ, Wang ZY, Zeng J (2020) Land use transitions and the associated impacts on ecosystem services in the Middle Reaches of the Yangtze River Economic Belt in China based on the geo-informatic Tupu method. *Sci Total Environ* 701:134690.1-134690.13
- Chen Y, Chen ZG, Xu GL, Tian ZQ (2016) Built-up land efficiency in urban China: Insights from the General Land Use Plan (2006–2020). *Habitat Int* 51:31–38
- Chen Y, Zhu MK, Lu JL, Zhou Q, Ma WB (2020) Evaluation of ecological city and analysis of obstacle factors under the background of high-quality development: Taking cities in the Yellow River Basin as examples. *Ecol Indic* 118:106771
- Chen YH, Xu MH, Wang ZL, Gao P, Lai CG (2021) Applicability of two satellite-based precipitation products for assessing rainfall erosivity in China. *Sci Total Environ* 757:143975
- Chen YM, Yao MR, Zhao QQ, Chen ZJ, Jiang PH, Li MC, Chen D (2021) Delineation of a basic farmland protection zone based on spatial connectivity and comprehensive quality evaluation: A case study of Changsha City, China. *Land Use Policy* 101:105145
- Cheng QW, Jiang PH, Cai LY, Shan JX, Zhang YQ, Wang LY, Li MC, Li FX, Zhu AX, Chen D (2017) Delineation of a permanent basic farmland protection area around a city centre: Case study of Changzhou City, China. *Land Use Policy* 60:73–89
- Chuai XW, Huang XJ, Lai L, Wang WJ, Peng JW, Zhao RQ (2013) Land use structure optimization based on carbon storage in several regional terrestrial ecosystems across China. *Environ Sci Policy* 25:50–61
- Chuai XW, Huang XJ, Wang WJ, Zhao RQ, Zhang M, Wu CY (2015) Land use, total carbon emission's change and low carbon land management in Coastal Jiangsu, China. *J Clean Prod* 103:77–86
- Clark M, Tilman D (2017) Comparative analysis of environmental impacts of agricultural production systems, agricultural input efficiency, and food choice. *Environ Res Lett* 12:064016
- Coderoni S, Esposti R (2018) CAP payments and agricultural GHG emissions in Italy A Farm-Level Assessment. *Sci Total Environ* 627:427–437
- Cremades R, Rothausen S, Conway D, Zou XX, Wang JX, Li Y (2016) Co-benefits and trade-offs in the water-energy nexus of irrigation modernization in China. *Environ. Res Lett* 11:054007
- Cui Y, Khan SU, Deng Y, Zhao MJ, Hou MY (2021) Environmental improvement value of agricultural carbon reduction and its spatiotemporal dynamic evolution: Evidence from China. *Sci Total Environ* 754:142170
- Dahal RP, Aguilar FX, McGarvey RG, Becker D, Abt KL (2020) Localized economic contributions of renewable wood-based biopower generation. *Energy Econ* 91:104913
- Dai X, Wang LC, Huang CB, Fang LL, Wang SQ, Wang LZ (2020) Spatio-temporal variations of ecosystem services in the urban agglomerations in the middle reaches of the Yangtze River, China. *Ecol Indic* 115:106394
- Deng XZ, Huang JK, Rozelle S, Zhang JP, Li ZH (2015) Impact of urbanization on cultivated land changes in China. *Land Use Policy* 45:1–7
- Ding, L.L., Wu, M.L., Jiao, Z., Nie, Y.Y., 2021. The positive role of trade openness in industrial green total factor


- productivity-provincial evidence from China. *Environ Sci Pollut Res*
- Dissanayake S, Mahadevan R, Asafu-Adjaye J (2020) Evaluating the efficiency of carbon emissions policies in a large emitting developing country. *Energy Policy* 136:111080.1-111080.11
- Doddabasawa, Chittapur BM, Murthy MM (2020) Comparison of carbon footprint of traditional agroforestry systems under rainfed and irrigated ecosystems. *Agrofor Syst* 94:465–475
- Dong F, Long RY, Bian ZF, Xu XH, Yu BL, Wang Y (2017) Applying a Ruggiero three-stage super-efficiency DEA model to gauge regional carbon emission efficiency: evidence from China. *Nat Hazards* 87:1453–1468
- Dong SK, Shang ZH, Gao JX, Boone RB (2020) Enhancing sustainability of grassland ecosystems through ecological restoration and grazing management in an era of climate change on Qinghai-Tibetan Plateau. *Agric Ecosyst Environ* 287:106684
- Elahi E, Abid M, Zhang LQ, ulHaq S, Sahito JGM (2018) Agricultural advisory and financial services; farm level access, outreach and impact in a mixed cropping district of Punjab, Pakistan. *Land Use Policy* 71:249–260
- Fan MS, Shen JB, Yuan LX, Jiang RF, Chen XP, Davies WJ, Zhang FS (2012) Improving crop productivity and resource use efficiency to ensure food security and environmental quality in China. *J Exp Bot* 63:13–24
- Faust S, Koch HJ, Joergensen RG (2019) Respiration response to different tillage intensities in transplanted soil columns. *Geoderma* 352:289–297
- Fox JA, Adriaanse P, Stacey NT (2019) Greenhouse energy management: The thermal interaction of greenhouses with the ground. *J Clean Prod* 235:288–296
- Fukumoto T, Muto I (2012) Rebalancing China's Economic Growth: Some Insights from Japan's Experience. *China World Econ* 20(1):62–82
- Garba MD, Usman M, Khan S, Shehzad F, Galadima A, Ehsan MF, Ghanem AS, Humayun M (2021) CO₂ towards fuels: A review of catalytic conversion of carbon dioxide to hydrocarbons. *J Environ Chem Eng* 9:104756
- Garg S, Li MR, Weber AZ, Ge L, Li LY, Rudolph V, Wang GX, Rufford TE (2020) Advances and challenges in electrochemical CO₂ reduction processes: an engineering and design perspective looking beyond new catalyst materials. *J Mater Chem A* 8:1511–1544
- Garnier J, Le Noe J, Marescaux A, Sanz-Cobena A, Lassaletta L, Silvestre M, Thieu V, Billen G (2019) Long-term changes in greenhouse gas emissions from French agriculture and livestock (1852–2014): From traditional agriculture to conventional intensive systems. *Sci Total Environ* 660:1486–1501
- Ge DZ, Long HL, Zhang YG, Ma L, Li TT (2018) Farmland transition and its influences on grain production in China. *Land Use Policy* 70:94–105
- Golosov VN, Collins AL, Dobrovolskaya NG, Bazhenova OI, Ryzhov YV, Sidorchuk AY (2021) Soil loss on the arable lands of the forest-steppe and steppe zones of European Russia and Siberia during the period of intensive agriculture. *Geoderma* 381:114678
- Gonzalez-Sanchez EJ, Ordonez-Fernandez R, Carbonell-Bojollo R, Veroz-Gonzalez O, Gil-Ribes JA (2012) Meta-analysis on atmospheric carbon capture in Spain through the use of conservation agriculture. *Soil Tillage Res* 122:52–60
- Grassini P, Cassman KG (2012) High-yield maize with large net energy yield and small global warming intensity. *Proc Natl Acad Sci USA* 109:1074–1079
- Guo SS, Wang YH, Huang J, Dong JH, Zhang J (2021) Decoupling and Decomposition Analysis of Land Natural Capital Utilization and Economic Growth: A Case Study in Ningxia Hui Autonomous Region, China. *Int J Environ Res Public Health* 18:646
- Han HB, Zhang XY (2020) Exploring environmental efficiency and total factor productivity of cultivated land use in China. *Sci Total Environ* 726:138434
- Huang A, Xu YQ, Liu C, Lu LH, Zhang YB, Sun PL, Zhou GY, Du T, Xiang Y (2019) Simulated town expansion under ecological constraints: A case study of Zhangbei County, Hebei Province, China. *Habitat Int* 91:101986
- Huang, C.K., Lin, F.Y., Chu, D.P., Wang, L.L., Liao, J.W., Wu, J.Q., 2021. Coupling Relationship and Interactive Response between Intensive Land Use and Tourism Industry Development in China's Major Tourist Cities. *Land* 10(7).
- Ibrahim MD, Alola AA, Ferreira DC (2021) A two-stage data envelopment analysis of efficiency of social-ecological systems: Inference from the sub-Saharan African countries. *Ecol Indic* 123:107381
- Jaafar HH, Ahmad FA (2020) Time series trends of Landsat-based ET using automated calibration in METRIC and SEBAL: The Bekaa Valley, Lebanon. *Remote Sens Environ* 238:111034
- Khoshnevisan B, Rafiee S, Omid M, Mousazadeh H (2013) Applying data envelopment analysis approach to improve energy efficiency and reduce GHG (greenhouse gas) emission of wheat production. *Energy* 58:588–593
- Kondo M, Patra PK, Sitch S, Friedlingstein P, Poulter B, Chevallier F, Ciais P, Canadell JG, Bastos A, Lauerwald R, Calle L, Ichii K, Anthoni P, Arneeth A, Haverd V, Jain AK, Kato E, Kautz M, Law RM, Lienert S, Lombardozi D, Maki T, Nakamura T, Peylin P, Rodenbeck C, Zhuravlev R, Saeki T, Tian HQ, Zhu D, Ziehn T (2020) State of the science in reconciling top-down and bottom-up approaches for terrestrial CO₂ budget. *Glob Chang Biol* 26(3):1068–1084
- Lal R (2020) The role of industry and the private sector in promoting the “4 per 1000” initiative and other negative emission technologies. *Geoderma* 378:114613
- Lemoine F, Poncet S, Unal D (2015) Spatial rebalancing and industrial convergence in China. *China Econ Rev* 34:39–63
- Li MQ, Liu SL, Sun YX, Liu YX (2021) Agriculture and animal husbandry increased carbon footprint on the Qinghai-Tibet Plateau during past three decades. *J Clean Prod* 278:123963
- Li, Q., Gao, M.F., Li, J.G., 2021. Carbon emissions inventory of farm size pig husbandry combining Manure-DNDC model and IPCC coefficient methodology. *J Clean Prod* 320.
- Li SC, Zhang H, Zhou XW, Yu HB, Li WJ (2020) Enhancing protected areas for biodiversity and ecosystem services in the Qinghai Tibet Plateau. *Ecosyst Serv* 43:101090
- Li W, Wei XP, Zhu RX, Guo KQ (2019a) Study on Factors Affecting the Agricultural Mechanization Level in China Based on Structural Equation Modeling. *Sustainability* 11:51
- Li YQ, Luo SL, Sun L, Kong DZ, Sheng JG, Wang K, Dong CW (2019b) A Green, Simple, and Rapid Detection for Amaranth in Candy Samples Based on the Fluorescence Quenching of Nitrogen-Doped Graphene Quantum Dots. *Food Anal Methods* 12:1658–1665
- Liang XY, Li YB (2020) Identification of spatial coupling between cultivated land functional transformation and settlements in Three Gorges Reservoir Area, China. *Habitat Int* 104:102236
- Liao T, Li D, Wan Q (2020) Tradeoff of Exploitation-protection and Suitability Evaluation of Low-slope hilly from the perspective of “production-living-ecological” optimization. *Phys Chem Earth Parts A/B/C* 120:102943
- Liou JL, Wu PI (2011) Will economic development enhance the energy use efficiency and CO₂ emission control efficiency? *Expert Syst Appl* 38(10):12379–12387
- Liu CY, Dou XT, Li JF, Cai LPA (2020a) Analyzing government role in rural tourism development: An empirical investigation from China. *J Rural Stud* 79:177–188
- Liu GS, Wang HM, Cheng YX, Zheng B, Lu ZL (2016) The impact of rural out-migration on arable land use intensity: Evidence from mountain areas in Guangdong, China. *Land Use Policy* 59:569–579

- Liu J, Jin XB, Xu WY, Gu ZM, Yang XH, Ren J, Fan YT, Zhou YK (2020) A new framework of land use efficiency for the coordination among food, economy and ecology in regional development. *Sci Total Environ* 710:135670
- Liu K, Qiao YR, Shi T, Zhou Q (2021) Study on coupling coordination and spatiotemporal heterogeneity between economic development and ecological environment of cities along the Yellow River Basin. *Environ Sci Pollut Res* 28:6898–6912
- Liu YS, Zou LL, Wang YS (2020) Spatial-temporal characteristics and influencing factors of agricultural eco-efficiency in China in recent 40 years. *Land Use Policy* 97:104794
- Liu, S.G., Bliss, N., Sundquist, E., Huntington, T.G., 2003. Modeling carbon dynamics in vegetation and soil under the impact of soil erosion and deposition. *Global Biogeochem Cy* 17(2).
- Lou HZ, Yang ST, Zhao CS, Wang ZW, Shi LH, Wu LN, Dong GT, Cai MY, Hao FH, Sun Y (2017) Using a nitrogen-phosphorus ratio to identify phosphorus risk factors and their spatial heterogeneity in an intensive agricultural area. *Catena* 149:426–436
- Lu H, Xie HL, Lv TG, Yao GR (2019) Determinants of cultivated land recuperation in ecologically damaged areas in China. *Land Use Policy* 81:160–166
- Lv XZ, Zuo ZG, Ni YX, Sun J, Wang HN (2019) The effects of climate and catchment characteristic change on streamflow in a typical tributary of the Yellow River. *Sci Rep* 9:14535
- Ma MD, Ma X, Cai WG, Cai W (2019) Carbon-dioxide mitigation in the residential building sector: A household scale-based assessment. *Energy Convers Manage* 198:111915
- Maraseni T, An-Vo DA, Mushtaq S, Reardon-Smith K (2021) Carbon smart agriculture: An integrated regional approach offers significant potential to increase profit and resource use efficiency, and reduce emissions. *J Clean Prod* 282:124555
- Matzek, V., Lewis, D., O'Geen, A., Lennox, M., Hogan, S.D., Feirer, S.T., Eviner, V., Tate, K.W., 2020. Increases in soil and woody biomass carbon stocks as a result of rangeland riparian restoration. *Carbon Balance Manage* 15.
- May S, Kocabiyik H (2019) Design and development of an electronic drive and control system for micro-granular fertilizer metering unit. *Comput Electron Agric* 162:921–930
- Meijboom FLB, Stafleu FR (2016) Farming ethics in practice: from freedom to professional moral autonomy for farmers. *Agr Hum Values* 33:403–414
- Ni B, Zhang W, Xu XC, Wang LG, Bol R, Wang KY, Hu ZJ, Zhang HX, Meng FQ (2021) Exponential relationship between N₂O emission and fertilizer nitrogen input and mechanisms for improving fertilizer nitrogen efficiency under intensive plastic-shed vegetable production in China: A systematic analysis. *Agric Ecosyst Environ* 312:107353
- Pan XX, Chen ML, Ying LM, Zhang FF (2020) An empirical study on energy utilization efficiency, economic development, and sustainable management. *Environ Sci Pollut Res* 27(12):12874–12881
- Paramesh V, Arunachalam V, Nikkhah A, Das B, Ghnimi S (2018) Optimization of energy consumption and environmental impacts of arecanut production through coupled data envelopment analysis and life cycle assessment. *J Clean Prod* 203:674–684
- Pendrill F, Persson UM, Godar J, Kastner T, Moran D, Schmidt S, Wood R (2019) Agricultural and forestry trade drives large share of tropical deforestation emissions. *Global Environ Chang* 56:1–10
- Pratt B, Chang HJ (2012) Effects of land cover, topography, and built structure on seasonal water quality at multiple spatial scales. *J Hazard Mater* 209:48–58
- Qi DY, Apolzan JW, Li R, Roe BE (2020) Unpacking the decline in food waste measured in Chinese households from 1991 to 2009. *Resour Conserv Recycl* 160:104893
- Ricardo, D., 2001. *On the Principles of Political Economy and Taxation*. Batoche Books, Ontario. (First published in 1817).
- Rocha A, Goncalves E, Almeida E (2019) Agricultural technology adoption and land use: evidence for Brazilian municipalities. *J Land Use Sci* 14:320–346
- Rodriguez-Galiano VF, Chica-Olmo M, Abarca-Hernandez F, Atkinson PM, Jeganathan C (2012) Random Forest classification of Mediterranean land cover using multi-seasonal imagery and multi-seasonal texture. *Remote Sens Environ* 121:93–107
- Sarkodie SA, Ozturk I (2020) Investigating the Environmental Kuznets Curve hypothesis in Kenya: A multivariate analysis. *Renew Sust Energy Rev* 117:109481
- Shang ZH, Cao JJ, Degen AA, Zhang DW, Long RJ (2019) A four year study in a desert land area on the effect of irrigated, cultivated land and abandoned cropland on soil biological, chemical and physical properties. *CATENA* 175:1–8
- Shi WJ, Tao FL, Liu JY (2013) Changes in quantity and quality of cropland and the implications for grain production in the Huang-Huai-Hai Plain of China. *Food Secur* 5(1):69–82
- Some S, Roy J, Ghose A (2019) Non-CO₂ emission from cropland based agricultural activities in India: A decomposition analysis and policy link. *J Clean Prod* 225:637–646
- Song, C.Z., Yin, G.W., Lu, Z.L., Chen, Y.B., 2021. Industrial ecological efficiency of cities in the Yellow River Basin in the background of China's economic transformation: spatial-temporal characteristics and influencing factors. *Environ Sci Pollut Res*
- Song L, Zhou XL (2021) How does industrial policy affect manufacturing carbon emission? Evidence from Chinese provincial sub-sectoral data. *Environ Sci Pollut Res* 28(43):61608–61622
- Su B, Xiao CJ, Deka R, Seielstad MT, Kangwanpong D, Xiao JH, Lu DR, Underhill P, Cavalli-Sforza L, Chakraborty RJ, Jin L (2000) Y chromosome haplotypes reveal prehistorical migrations to the Himalayas. *Hum Genet* 107(6):582–590
- Su MR, Fath BD (2012) Spatial distribution of urban ecosystem health in Guangzhou, China. *Ecol Indic* 15:122–130
- Sun YF, Ma AB, Su HR, Su SL, Chen F, Wang W, Weng M (2020) Does the establishment of development zones really improve industrial land use efficiency? Implications for China's high-quality development policy. *Land Use Policy* 90:104265
- Tercan E, Dereli MA (2020) Development of a land suitability model for citrus cultivation using GIS and multi-criteria assessment techniques in Antalya province of Turkey. *Ecol Indic* 117:106549
- Tian PP, Li D, Lu HW, Feng SS, Nie QW (2021) Trends, distribution, and impact factors of carbon footprints of main grains production in China. *J Clean Prod* 278:123347
- Vallejo M, Casas A, Perez-Negron E, Moreno-Calles AI, Hernandez-Ordenez O, Tellez O, Davila P (2015) Agroforestry systems of the lowland alluvial valleys of the Tehuacan-Cuicatlan Biosphere Reserve: an evaluation of their biocultural capacity. *J Ethnobiol Ethnomed* 11:1–19
- Wang GC, Luo ZK, Wang EL, Zhang W (2018a) Reducing greenhouse gas emissions while maintaining yield in the croplands of Huang-Huai-Hai Plain, China. *Agric for Meteorol* 260:80–94
- Wang, J., Wu, H.Q., Chen, Y., 2020. Made in China 2025 and manufacturing strategy decisions with reverse QFD. *Int J Prod Econ* 224
- Wang, Y., Feng, Y.N., Zuo, J., Rameezdeen, R., 2019. From "Traditional" to "Low carbon" urban land use: Evaluation and obstacle analysis. *Sustain Cities Soc* 51
- Wang ZF, Cheng WC, Wang YQ (2018b) Investigation into geohazards during urbanization process of Xi'an, China. *Nat Hazards* 92(3):1937–1953
- Wang ZS, Liu L, Xu Z, Li Z, Li Y (2015) Research on a Carbon Reduction Optimization Model for a Megalopolis Based on Land-Use Planning and ICCLP Method. *Pol J Environ Stud* 24(1):347–354
- Wanke P, Chen ZF, Zheng X, Antunes J (2020) Sustainability efficiency and carbon inequality of the Chinese transportation system: A Robust Bayesian Stochastic Frontier Analysis. *J Environ Manage* 260:110163

- Wu D, Yan DH, Yang GY, Wang XG, Xiao WH, Zhang HT (2013) Assessment on agricultural drought vulnerability in the Yellow River basin based on a fuzzy clustering iterative model. *Nat Hazards* 67(2):919–936
- Wu, H.W., Guo, B., Fan, J.F., Yang, F., Han, B.M., Wei, C.X., Lu, Y.F., Zang, W.Q., Zhen, X.Y., Meng, C., 2021. A novel remote sensing ecological vulnerability index on large scale: A case study of the China-Pakistan Economic Corridor region. *Ecol Indic* 129
- Wu YF, Feng WL, Zhou Y (2019) Practice of barren hilly land consolidation and its impact: A typical case study from Fuping County, Hebei Province of China. *J Geogr Sci* 29:762–778
- Wu YZ, Shan LP, Guo Z, Peng Y (2017) Cultivated land protection policies in China facing 2030: Dynamic balance system versus basic farmland zoning. *Habitat Int* 69:126–138
- Xia LL, Zhang Y, Wu Q, Liu LM (2017) Analysis of the ecological relationships of urban carbon metabolism based on the eight nodes spatial network model. *J Clean Prod* 140:1644–1651
- Xiao Y, Guo B, Lu YF, Zhang R, Zhang DF, Zhen XY, Chen ST, Wu HW, Wei CX, Yang LA, Zhang Y, Zang WQ, Huang XZ, Sun GQ, Wang Z (2021) Spatial-temporal evolution patterns of soil erosion in the Yellow River Basin from 1990 to 2015: impacts of natural factors and land use change. *Geomatics. Nat Hazards Risk* 12:103–122
- Xie HL, He YF, Zou JL, Wu Q (2016) Spatio-temporal difference analysis of cultivated land use intensity based on emergy in the Poyang Lake Eco-economic Zone of China. *J Geogr Sci* 26:1412–1430
- Xie HL, Huang YQ, Choi Y, Shi JY (2021) Evaluating the sustainable intensification of cultivated land use based on emergy analysis. *Technol Forecast Soc Change* 165:120449
- Xie HL, Liu GY (2015) Spatiotemporal differences and influencing factors of multiple cropping index in China during 1998–2012. *J Geogr Sci* 25:1283–1297
- Xie HL, Zhai QL, Wang W, Yu JL, Lu FC, Chen QR (2018) Does intensive land use promote a reduction in carbon emissions? Evidence from the Chinese industrial sector. *Resour Conserv Recycl* 137:167–176
- Xu Q, Yang R (2019) The sequential collaborative relationship between economic growth and carbon emissions in the rapid urbanization of the Pearl River Delta. *Environ Sci Pollut Res* 26(29):30130–30144
- Xu WY, Jin XB, Liu J, Zhou YK (2020) Impact of cultivated land fragmentation on spatial heterogeneity of agricultural agglomeration in China. *J Geogr Sci* 30:1571–1589
- Yan SQ, Peng JC, Wu Q (2020) Exploring the non-linear effects of city size on urban industrial land use efficiency: A spatial econometric analysis of cities in eastern China. *Land Use Policy* 99:104944
- Yang B, Chen X, Wang ZQ, Li WD, Zhang CR, Yao XW (2020) Analyzing land use structure efficiency with carbon emissions: A case study in the Middle Reaches of the Yangtze River, China. *J Clean Prod* 274:123076
- Yang GM, Zhang F, Zhang FT, Ma DL, Gao L, Chen Y, Luo Y, Yang Q (2021) Spatiotemporal changes in efficiency and influencing factors of China's industrial carbon emissions. *Environ Sci Pollut Res* 28(27):36288–36302
- Yang YZ, Cheng ZJ, Li WY, Yao L, Li ZY, Luo WH, Yuan ZJ, Zhang J, Zhang JZ (2016) The emergence, development and regional differences of mixed farming of rice and millet in the upper and middle Huai River Valley, China. *Sci China Earth Sci* 59:1779–1790
- Yin LC, Feng XM, Fu BJ, Wang S, Wang XF, Chen YZ, Tao FL, Hu J (2021) A coupled human-natural system analysis of water yield in the Yellow River basin, China. *Sci Total Environ* 762:143141
- Zhang CQ, Chen PY (2021) Industrialization, urbanization, and carbon emission efficiency of Yangtze River Economic Belt-empirical analysis based on stochastic frontier model. *Environ Sci Pollut Res* 28(47):66914–66929
- Zhang, D., Geng, X.L., Chen, W.X., Fang, L., Yao, R., Wang, X.R., Zhou, X., 2021. Inconsistency of Global Vegetation Dynamics Driven by Climate Change: Evidences from Spatial Regression. *Remote Sens-basel* 13(17).
- Zhang D, Wang XR, Qu LP, Li SC, Lin YP, Yao R, Zhou X, Li JY (2020) Land use/cover predictions incorporating ecological security for the Yangtze River Delta region, China. *Ecol Indic* 119:106841
- Zhang K, Xie XH, Zhu BW, Meng SS, Yao Y (2019) Unexpected groundwater recovery with decreasing agricultural irrigation in the Yellow River Basin. *Agric Water Manag* 213:858–867
- Zhang YS, Lu X, Liu BY, Wu DT, Fu G, Zhao YT, Sun PL (2021) Spatial relationships between ecosystem services and socioecological drivers across a large-scale region: A case study in the Yellow River Basin. *Sci Total Environ* 766:142480
- Zhang ZT, Xu EQ, Zhang HQ (2021) Complex network and redundancy analysis of spatial-temporal dynamic changes and driving forces behind changes in oases within the Tarim Basin in north-western China. *Catena* 201:105216
- Zhao XL, Yin HT (2011) Industrial relocation and energy consumption: Evidence from China. *Energy Policy* 39(5):2944–2956
- Zhou SD, Mueller F, Burkhard B, Cao XJ, Hou Y (2013) Assessing Agricultural Sustainable Development Based on the DPSIR Approach: Case Study in Jiangsu, China. *J Integr Agr* 12:1292–1299
- Zhou, Y.X., Liu, W.L., Lv, X.Y., Chen, X.H., Shen, M.H., 2019. Investigating interior driving factors and cross-industrial linkages of carbon emission efficiency in China's construction industry: Based on Super-SBM DEA and GVAR model. *J Clean Prod* 241.
- Zhou Y, Li XH, Liu YS (2020) Land use change and driving factors in rural China during the period 1995–2015. *Land Use Policy* 99:105048
- Zhu, Y., Du, W.B., Zhang, J.T., 2021. Does industrial collaborative agglomeration improve environmental efficiency? Insights from China's population structure. *Environ Sci Pollut Res*
- Zhu YC, Waqas MA, Li YE, Zou XX, Jiang DF, Wilkes A, Qin XB, Gao QZ, Wan YF, Hasbagan G (2018) Large-scale farming operations are win-win for grain production, soil carbon storage and mitigation of greenhouse gases. *J Clean Prod* 172:2143–2152

Publisher's note Springer Nature remains neutral with regard to jurisdictional claims in published maps and institutional affiliations.

Authors and Affiliations

Xiao Zhou^{1,2} · Juan Yu^{1,2} · Jiangfeng Li^{1,2} · Shicheng Li^{1,2} · Dou Zhang³ · Di Wu^{1,2} · Sipei Pan^{1,2} · Wanxu Chen^{4,5,6,7} 

¹ Department of Land Resources Management, School of Public Administration, China University of Geosciences, Wuhan 430074, China

² Key Laboratory of Rule of Law Research, Ministry of Natural Resources, Wuhan 430074, China

³ Department of Environmental Science and Engineering, Fudan University, Shanghai 200438, China

⁴ Department of Geography, School of Geography and Information Engineering, China University of Geosciences, Wuhan 430074, China

⁵ Research Center for Spatial Planning and Human-Environmental System Simulation, China University of Geosciences, Wuhan 430074, China

⁶ State Key Laboratory of Earth Surface Processes and Resource Ecology, Beijing Normal University, Beijing 100875, China

⁷ School of Geography and Information Engineering, East Lake New Technology Development Zone, China University of Geosciences, No. 68, Jincheng Street, Wuhan, Hubei Province 430078, People's Republic of China